Archival Report

Biological Psychiatry: GOS

Diminished Social Memory and Hippocampal Correlates of Social Interactions in Chronic Social Defeat Stress Susceptibility

Amanda Larosa, Tian Rui Zhang, Alice S. Wong, Cyrus Y.H. Fung, Xiong Ling Yun (Jenny) Long, Prabhjeet Singh, Benjamin C.M. Fung, and Tak Pan Wong

ABSTRACT

BACKGROUND: Susceptibility to chronic stress has been associated with depression, a mood disorder that highly implicates the hippocampus. Hippocampal contribution to stress susceptibility has been supported by findings in mice following chronic social defeat stress (CSDS). However, little is known about the role of hippocampal activity in determining the development of stress susceptibility.

METHODS: We used the UCLA Miniscope to longitudinally measure the activity of dorsal CA1 hippocampal neurons during CSDS. In addition to examining the representation of social information by these neurons, we compared social memory in mice that were either susceptible or resilient to CSDS.

RESULTS: We observed more stable dorsal CA1 correlates of social interaction and social memory in CSDS-resilient mice. Such changes were absent in CSDS-susceptible mice and accompanied by greater social memory impairments.

CONCLUSIONS: CSDS susceptibility may be supported by hippocampal social cognitive processes, as reflected in diminished hippocampal representations of social information and greater impairment in social memory in suspectible compared with resilient mice.

https://doi.org/10.1016/j.bpsgos.2025.100455

Chronic stress represents a risk factor for depression, a debilitating mood disorder impacting approximately 280 million individuals globally (1,2). The hippocampus is highly implicated in depression (3). Differential hippocampal changes have been identified in stress-exposed groups of people who go on to develop depression-like features, termed susceptible, compared with those who seem to be resilient to stress. Hippocampal hyperactivity is among the observed changes in both patients with depression responding to negative stimuli and mouse models of depression (4–6). Using a social stressor called chronic social defeat stress (CSDS) to separate mice into susceptible and resilient populations (7), we found that more hippocampal CA1 neurons were reactivated by the CSDS experience in susceptible mice (8). Changes in hippocampal activity invariably led to alterations in its function, including social cognition.

In humans, hippocampal activity during facial recognition correlates with how well participants report knowing a presented face (9). Findings from rodents support crucial roles of hippocampal subregions, including the dorsal CA2 and ventral CA3 and CA1 (10–12), in social memory. The dorsal CA1 (dCA1) subregion may also contribute to social information processing. dCA1 neurons preferentially fire according to a conspecific's location (13,14), which is likely crucial for informing the decision to engage in prosocial (e.g., approach) or antisocial (e.g., avoidance) behavior. The dCA1 is also essential for the recognition of social identity (15,16). Whether changes in dCA1 representation of social targets are related to social stressor susceptibility remains unclear.

To examine dCA1 representation of social information during CSDS, we longitudinally performed in vivo calcium imaging of dCA1 neurons throughout CSDS in male C57BL/6 mice. We hypothesized that the altered hippocampal activity in stress-susceptible mice would impact the processing of social information by the dCA1 and social memory.

METHODS AND MATERIALS

Animals

Male adult C57BL/6 mice (ages 2–3 months) and CD1 retired breeders (>6 months) were obtained (Charles River). Mice were housed under a 12-hour light/dark cycle (light on at 8:00 AM), with experiments being conducted during the light-on phase. All experiments were approved by the Facility Animal Care Committee at the Douglas Research Centre and followed the guidelines from the Canadian Council on Animal Care (protocol no.: DOUG-5935).

Surgeries

Under isoflurane, 253 nL of AAV2/9-SYN-GCaMP6f virus at 23 nL/s was stereotaxically injected in the dCA1 (bregma:

ISSN: 2667-1743

AP: −1.60; ML: +1.70; DV: −1.40 or AP: −1.90; ML: +1.40; DV: −1.10; the coordinates achieved comparable results). The volume was separated into 5 injections, with interinjection intervals of 30 seconds and the pipette remaining in place for a total of 10 minutes prior to being withdrawn. One week later, a gradient refractive index lens (pitch: 0.25, diameter: 1.8 mm, length: 4 mm; Edmund Optics) was implanted above the injection site, with the cortical tissue above aspirated. The gradient refractive index lens was fixed in position using cyanoacrylate and dental cement. Three weeks later, a baseplate for attaching the miniscope was cemented on the head surface.

Chronic Social Defeat Stress

C57BL/6 mice were attacked by CD1 aggressors during CSDS (8). CSDS consisted of 8 episodes of defeat. Mice were attacked daily, with up to 12 attacks occurring during a maximum period of 5 minutes. Following defeat, C57BL/6 mice were housed with the CD1 aggressor for 24 hours. A perforated partition separated defeated mice from aggressors during cohousing to allow for the presence of sensory stressors. A new CD1 aggressor was used in each defeat episode to prevent habituation from the same aggressor. Control nonstressed C57BL/6 mice were weighed daily and pair-housed for 8 days. After CSDS or pair housing, social behaviors of stressed and control mice were examined in a social interaction test (SIT) (17).

The SIT consisted of two 150-second sessions in an open field (44 × 44 × 44 cm). An empty perforated enclosure (10 × 5 × 30 cm) was placed in the center of the north side of the open field during session 1. During session 2, a novel CD1 mouse was placed in the enclosure. Both sessions were performed under ambient red light and static white noise (60 dB). Time spent in the interaction zone (10 cm around the enclosure) during the SIT was estimated using TopScan LITE (Clever System Inc.). The social interaction ratio was calculated as interaction time session 2 (CD1)/interaction time session 1 (empty). Stressed mice with a social interaction ratio >1 were considered resilient. All other stressed mice were considered susceptible mice. Gradient refractive index lens placement was histologically confirmed after the SIT.

Social Memory Tests

Testing took place 1 day prior to the start of CSDS or 5 days post-CSDS. For both pre- and post-CSDS studies, subject mice were tested in three 8-minute open field sessions: 1) 2 empty cups, 2) 1 empty cup and 1 cup with novel CD1 A, and 3) 1 cup with now-familiar CD1 A and novel CD1 B. The intersession durations for pre- and post-CSDS studies were 1 minute and 2 hours, respectively. Cup position was counterbalanced. For post-CSDS studies, another open field session with the familiar CD1 A and an empty cup was added the next day. Time spent exploring each cup was measured. All sessions were performed under ambient red light and static white noise.

In Vivo Calcium Imaging

Using the UCLA Miniscope (version 3), we conducted in vivo calcium imaging of dCA1 neurons during cohousing with a conspecific or an aggressor after the second, fifth, and eighth episode of CSDS and the SIT. Mice were separated from the cohoused control or aggressor by a perforated partition.

Recordings were performed via the Miniscope-DAQ-QT-Software (Aharoni-Lab, GitHub). These recordings were concatenated, motion-corrected, and aligned using NoRMCorre (18). Calcium signals from each cell segment were identified and extracted using Constrained Non-negative Matrix Factorization for microEndoscopic data (CNMF-E) (19). Overlapping segments (>60%) were discarded. The signal rising phase was binarized for estimating inferred spikes. Mouse body parts were annotated using *DeepLabCut* (20) to generate head position and heading direction vectors. All calcium and behavioral data were downsampled to 5 Hz.

Social Ensembles

dCA1 neurons were sorted according to their activity during social interaction bouts. Relative to the head of the social target, social interaction bouts were defined as <10 cm between the head of the subject mouse and <50° from the heading direction of the subject mouse. Only social interactions lasting at least 5 frames (1 second) were used. We identified neurons that were active during at least 40% of the social interaction bouts and calculated the mean activity of these neurons to construct the social ensemble vector. We found that the cosine similarity index (CSI) (21,22) of the social ensemble vector, which was calculated from the ensemble activity vector (C) and the social interaction bout vector (binary logical values of social interaction frames B; $CSI = 2B \bullet C/(|B|^2 \bullet |C|^2)$), was significantly higher than 95% of shuffled social interaction bout vectors (10,000 shuffled vectors). The social ensemble vector also showed poorer similarity with other behavioral vectors, such as subject mouse running speed and head direction.

Ensemble size was calculated by dividing the number of dCA1 neurons within a social ensemble by the total number of registered neurons within the same recording. Neuron reactivation was tracked using CellReg (23). Spatial information of dCA1 neurons in social ensembles was estimated (24) using $I = \int_x \lambda(x) log_2 \frac{\lambda(x)}{\lambda} p(x) dx$ (I = spatial information, x = spatial location, $\lambda(x)$ = mean firing rate of the cell at location x, $p(x)$ = probability of mice at location x, λ = overall mean firing rate of the cell), with spatial bins of 4 cm^2. Only frames with mice moving at >5 cm/s were included. MATLAB (version 2020a; The MathWorks, Inc.) codes for calcium imaging and spatial information calculations are shared at GitHub (https://github.com/tpwonglab/social-ensemble-analysis).

Statistical Analysis

All statistical analyses were performed using JMP version 15 and GraphPad version 10. Data normality was examined using the Shapiro-Wilk test. Two-way analysis of variance and post hoc Tukey tests were used to analyze calcium imaging data. For behavioral measures, 1-way analysis of variance and post hoc Tukey tests were used. Kruskal-Wallis and post hoc Wilcoxon tests were used for data that were not normally distributed. Student's t test and Mann-Whitney tests were

used for parametric and nonparametric pairwise comparisons. All data are presented as mean ± SEM.

RESULTS

Mouse Behaviors During CSDS Cohousing and SIT

We longitudinally monitored dCA1 activity in conjunction with social behavior using the miniscope to determine how neuronal correlates of social interactions evolved throughout CSDS in male mice. In vivo calcium imaging was performed during the cohousing that followed a defeat episode where both the C57BL/6 subject and CD1 aggressor (or nonstressed control mouse) were freely moving or during the SIT on day 9 (Figure 1A). To examine the long-term effect of CSDS on hippocampal activity, in vivo calcium imaging was performed 1-hour postdefeat. CSDS susceptibility and resilience were determined from behavioral performance in the SIT. Briefly, in the SIT, control and resilient mice spent more time in the area surrounding a CD1 mouse–containing enclosure, termed the interaction zone, than susceptible mice (Figure S1A, B). Susceptible mice spent more time in the corner zones (Figure S1C). No differences in the latency to first attack, attack number, or weight change during CSDS were observed between the 2 stressed groups (Figure S1D).

We compared the head distance ($Dist_{head}$) and the angle of heading direction ($Angle_{head}$) of subject mice to the neighboring social target's head during cohousing or the mouse-containing cup (center) in the SIT (Figure 1D). During cohousing, resilient mice maintained a smaller $Dist_{head}$ and $Angle_{head}$ with aggressors than control mice (Figure 1C), suggesting closer contacts between resilient mice and aggressors during cohousing. Moreover, behavioral analysis during the SIT revealed a shorter $Dist_{head}$ in resilient mice than susceptible mice (Figure 1D). The greater $Dist_{head}$ does not represent a lack of attention toward the aggressor by susceptible mice because unlike control mice, both susceptible and resilient mice displayed a between-session reduction of $Angle_{head}$. This suggests a smaller viewing angle in stressed mice toward the social target in the SIT. One-way analysis of variance of session 2 data from the SIT also revealed a group effect of greater $Dist_{head}$ and smaller $Angle_{head}$ in susceptible mice compared with resilient and control mice, respectively. Thus, during the SIT, resilient mice remained at closer proximity and positioned toward the CD1, while susceptible mice maintained a further distance but continued to face the CD1, potentially indicators of vigilance or social anxiety (25).

To specifically analyze social behavior during cohousing, interactions were defined as behavioral frames where the $Dist_{head}$ was <10 cm (D10), and the $Angle_{head}$ between mice was smaller than ±50° (A50; Figure 2A). Both stressed groups spent more time at D10 than control mice. We also compared the percentage of time that mice were situated at regions away

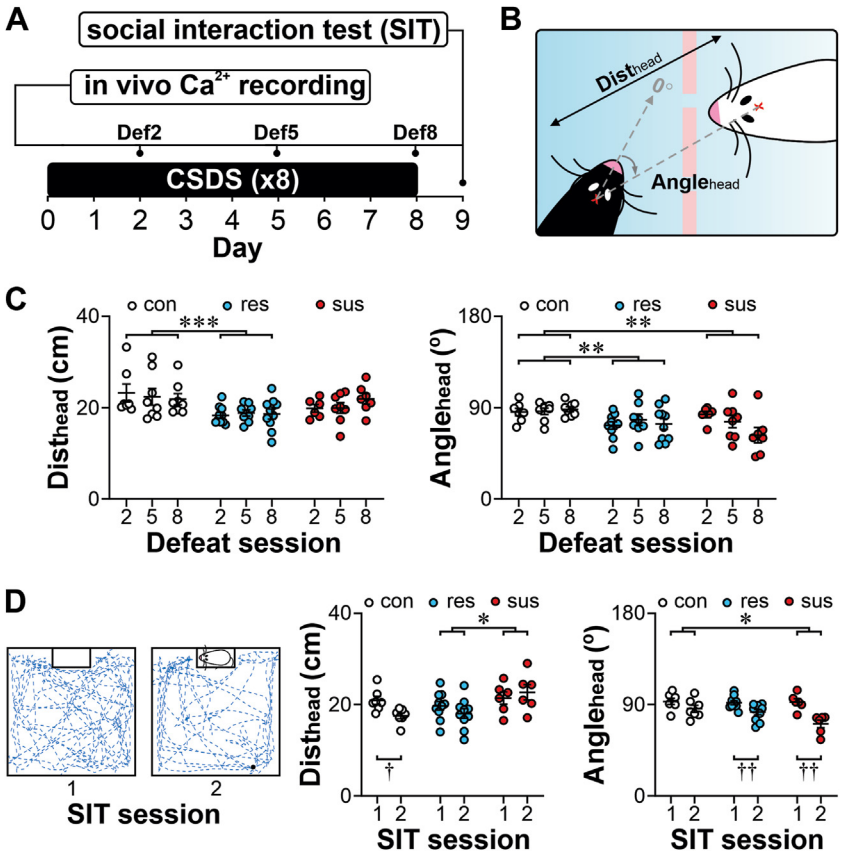

Figure 1. Differences in behavior between susceptible and resilient mice during cohousing post-CSDS and SIT. **(A)** Schematic of the experiment timeline. On day 1, CSDS began and was repeated daily for 8 consecutive days, with in vivo calcium imaging and behavior recordings conducted during the cohousing period that followed defeat days 2, 5, and 8. On day 9, the SIT was conducted along with in vivo calcium imaging recording. **(B)** Schematic demonstrating the relative $Dist_{head}$ and $Angle_{head}$ between the subject mouse (black) and its cohoused neighbor (white). **(C)** Average $Dist_{head}$ (left) and $Angle_{head}$ (right) following defeat sessions 2, 5, and 8 in con (white) (n = 7–8), res (blue) (n = 8–10), and sus (red) (n = 6–8) mice. **(D)** Left: schematic of session 1 (empty enclosure) and session 2 (CD1 mouse present in enclosure) of the SIT along with representative trace of subject trajectory (blue). Middle: $Dist_{head}$ during sessions 1 and 2 of the SIT. Right: $Angle_{head}$ during sessions 1 and 2 of the SIT (con: n = 7, res: n = 10, sus: n = 6). All data are expressed as mean ± SEM. $^{*}p < .05$, $^{**}p < .01$, $^{***}p < .001$, effect test of group with 2-way analysis of variance followed by Tukey's multiple comparisons test. $\dagger p < .05$, $\dagger\dagger p < .01$, paired t tests. $Angle_{head}$, head angle; con, control; CSDS, chronic social defeat stress; Def, defeat day; $Dist_{head}$, head distance; res, resilient; sus, susceptible.

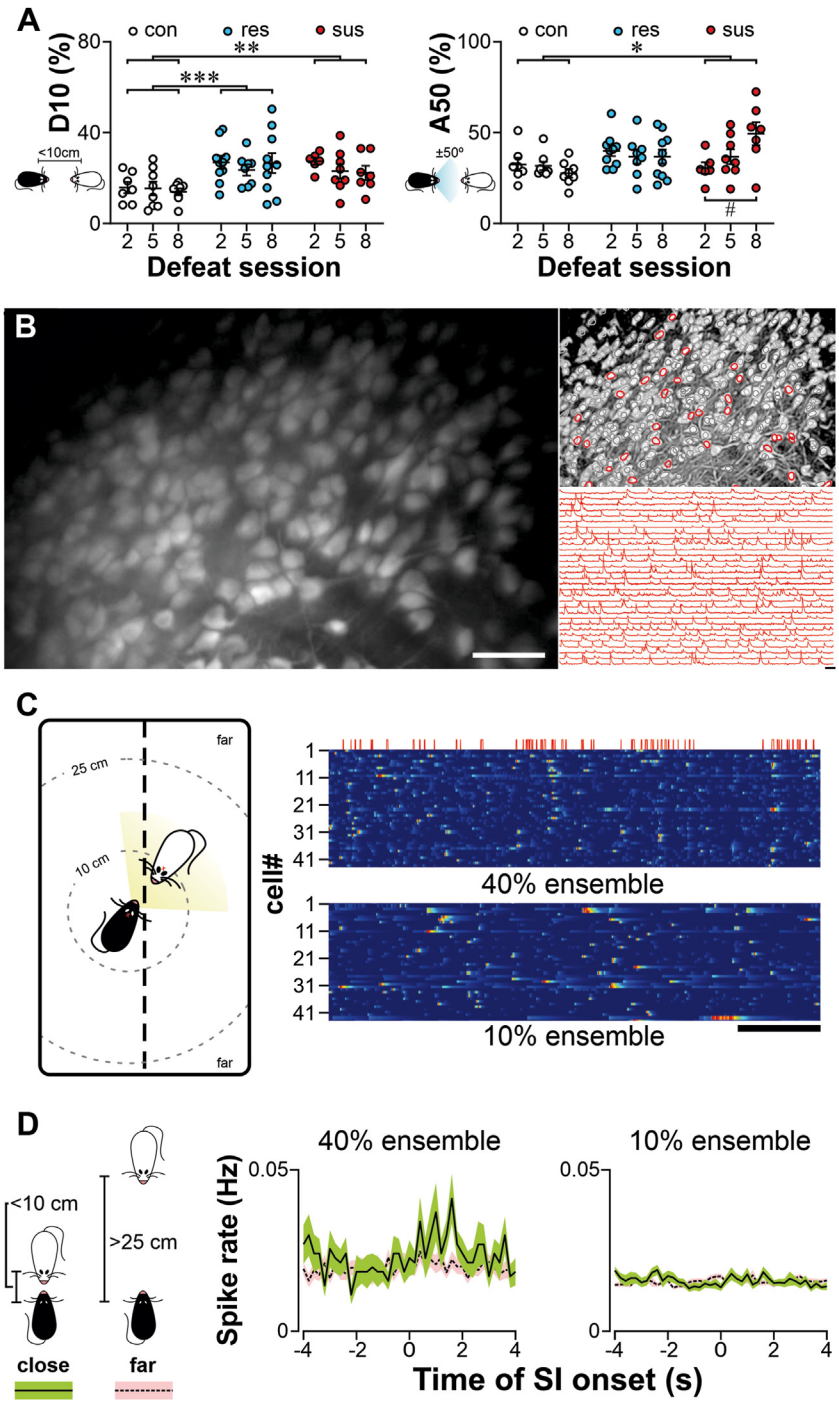

Figure 2. Identifying dorsal CA1 social ensembles. **(A)** Percentage of time spent at (left) head distance < 10 cm (D10) and (right) head angle < ±50° (A50) following defeat sessions 2, 5, and 8 in con (white) (n = 7–8), res (blue) (n = 8–10), and sus (red) (n = 6–8) mice. $^{*}p < .05$, $^{**}p < .01$, $^{***}p < .001$, effect test of group in 2-way analysis of variance followed by Tukey's multiple comparisons test. #$p < .05$, 1-way analysis of variance followed by Tukey's multiple comparisons test. **(B)** Left: dCA1 field of view demonstrating maximal activity from all active neurons expressing GCaMP6f in a recording session (scale bar = 20 μm). Right: micrograph from in vivo calcium imaging recording outlining individual dCA1 neurons with traces representing corresponding GCaMP6f fluorescent signals (scale bar = 1 minute). **(C)** Left: schematic representing interactions between a chronic social defeat stress subject mouse (black) and a CD1 aggressor (white) in the cohousing post-chronic social defeat stress. Right: inferred calcium activity for each dCA1 neuron sorted according to activity during social interaction bouts (red lines above raster plots). dCA1 social ensembles of neurons that were active during 40% (top) or 10% (bottom) of SI bouts (scale bar = 2 minutes). **(D)** Inferred calcium spike rate of (left) 40% ensemble and (right) 10% ensemble aligned according to close (<10 cm, green) and far (>25 cm, pink) social interaction onset. All data are expressed as mean ± SEM. con, control; dCA1, dorsal CA1; res, resilient; SI, social interaction; sus, susceptible.

from the social targets (when $Dist_{head}$ >25 cm) and found that resilient mice spent less time in this zone than control mice (Figure S2A). In terms of viewing angle, we found that susceptible mice remained at A50 longer than control mice (Figure 2A). A significant increase in time at A50 was also seen in susceptible mice between the second and eighth defeat session. Notably, when we compared the compass angle of subject mouse head direction (i.e., $Angle_{head}$ toward north = 0, unrelated to social targets), we observed no between-group differences (Figure S2B), suggesting that the increased time spent at A50 by susceptible mice was social target-related. Finally, while both stressed groups moved less than control

mice during recording, no difference between resilient and susceptible groups was found (Figure S2C). Together, these results indicate that nuances in social behavior seem to manifest throughout the course of defeat and result in diverging behavioral phenotypes in the SIT. These findings prompted us to further examine neuronal correlates of interactions (D10 and A50) between subject mice and social targets.

dCA1 Social Ensemble Activity Throughout CSDS and the SIT

Next, we determined whether variations in social behavior were accompanied by changes in hippocampal activity as measured by in vivo calcium imaging. Fluorescent calcium spikes were extracted and used as proxies for neuron activation (Figure 2B). We found an elevated inferred spike rate of dCA1 neurons in resilient compared with control mice (Figure S2D). These findings prompted us to identify dCA1 neurons that were active during social interaction. We extracted dCA1 population activity that was related to social interaction between the subject and target mice. This was done through the calculation of CSIs (26) between the mean inferred calcium spiking rate vector from a neuronal ensemble and the behavioral vector of social interaction bouts (D10 and A50). We identified ensembles of neurons that were active in 40% or 10% of all social interaction bouts and compared the activity of these neuronal ensembles (Figure 2C). An increase in the inferred calcium spike rate of the 40% ensemble was observed at the onset of close interactions ($Dist_{head} < 10$ cm) compared with far encounters ($Dist_{head} > 25$ cm) (Figure 2D). The inferred calcium spike rate of the 10% ensemble remained similar regardless of distance from the aggressor. These results indicated that the 40% ensemble reflected close social interactions with greater accuracy than the 10% ensemble. For all future analyses, the 40% ensemble was used and will henceforth be termed the social ensemble.

Across different sessions of CSDS cohousing, the inferred spiking rate of social ensemble neurons from all groups was greater when subjects were close to social targets than when they were far, except in susceptible mice after the second session of social defeat (Figure 3A). Although transient, the absence of social ensemble activity favoring close interactions in susceptible mice indicated that the neuronal representation of social interactions may be diminished in susceptible mice. Next, we quantified the level of congruence between their mean activity and social interactions that is represented by the CSI. Social ensembles showed a greater CSI in resilient mice than in both susceptible and control mice (Figure 3B), indicating that activity from social ensembles was better representative of interactions in resilience. Across CSDS sessions, social ensemble size, which represents the percentage of recorded neurons in social ensembles, was also greater in resilient than in control mice (Figure 3C). Considering that neuron reactivation is another signature relating activity to an experience (27), we used cell registration (23) to track the activity of the same individual neurons across different CSDS sessions. On average, approximately 50% of neurons reactivated across CSDS cohousing sessions (Figure 3D). Individual neuron reactivation may be initiated by several cues including contextual features; thus, we focused on social ensemble neuron reactivation. Approximately 50% to 70% of social ensemble neurons reactivated across CSDS cohousing sessions and remained comparable across groups. Next, we compared the reactivation of dCA1 neurons recorded in CSDS cohousing during the SIT (Figure 3E). We found that susceptible mice displayed reduced reactivation of social ensemble neurons compared with resilient and control mice. These findings suggest that in resilient mice, social ensemble neurons represent social interaction more consistently than they do in susceptible mice.

To determine whether variations in dCA1 social ensemble activity during CSDS cohousing and SIT could be attributed to parallel differences in interactions, we compared behavior in these recording sessions. The number of social bouts during CSDS cohousing was similar in the different mouse groups (Figure 4A). During social bouts, both defeated groups initiated approach less frequently and reacted to interactions with escape behavior more than control mice (Figure 4B). As expected, susceptible mice interacted less with the aggressors in the SIT. Together, observed differences in social ensemble activity during CSDS cohousing and the SIT are likely not explained by the dynamics of social behavior. Lastly, it is possible that dCA1 place-cell properties are responsible for the differences in ensemble activity that we observed in different mouse groups. We found that lower mean spatial information was carried by the social ensemble in both defeated groups compared with control mice during CSDS (Figure 4C). These findings seem to be congruent with the reported detrimental effect of stress on place-cell properties (28). Notably, social ensemble activity during cohousing was likely less sensitive to changes in place-cell properties because all mice during cohousing were freely moving and interacting at random locations. Interestingly, social ensembles carried more spatial information in susceptible than in resilient mice during the SIT. Whether this decrease in spatial information in a novel context is related to better social representation by these ensembles in resilient mice remains to be tested.

CSDS Impairs Social Memory With a Greater Effect in Susceptible Mice

The decreases in social ensemble fidelity in CSDS susceptibility may result in deficits in social memory. As shown by previous studies and our findings from another cohort of mice (Figures S3 and S4), avoidance in CSDS-susceptible mice is specific to the CD1 strain, suggesting a contribution from social memory for this aggressive strain. Using the preference for mice to interact with a novel conspecific (29), we characterized the impact of CSDS on social memory for the CD1 strain. We studied 3 different measures of social memory 4 days post-SIT (Figure 5A): short-term social memory for a familiar CD1 measured 2 hours later, social novelty memory for a novel CD1 versus a familiar CD1, and long-term social memory for a familiar CD1 measured 1 day later. In all cases, control mice displayed a decrease in interaction time when the social target was less novel (Figure 5B). Stressed mice showed impairment in social memory on all 3 measures compared with control mice. Interestingly, susceptible mice exhibited lower

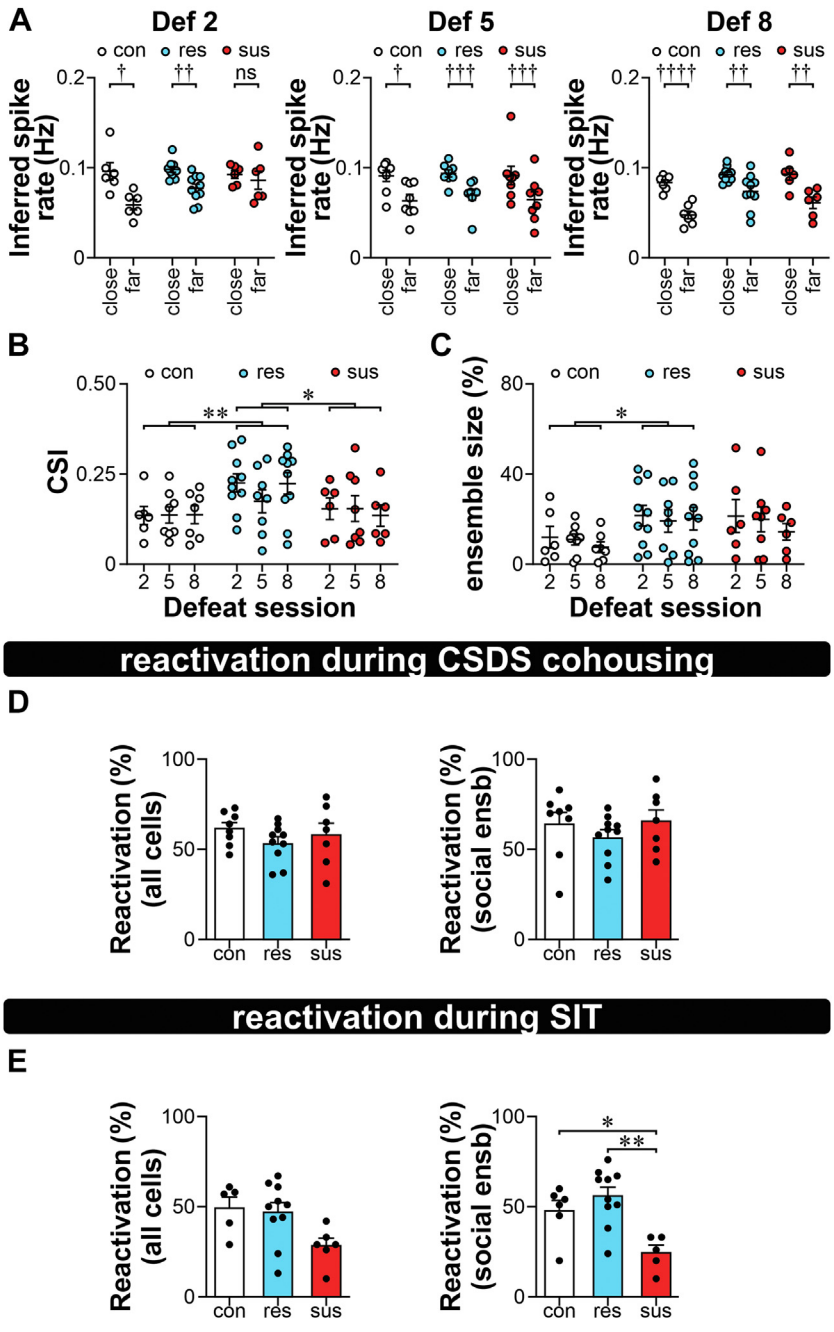

Figure 3. Dorsal CA1 social ensembles better represent interactions throughout CSDS in resilient mice. **(A)** Inferred calcium spike rate of social ensembles during close and far social interactions (con: $n = 6–8$, res: $n = 8–10$, sus: $n = 6–8$). †$p < .05$, ††$p < .01$, †††$p < .001$, ††††$p < .0001$, paired t tests. **(B)** Average CSI of social ensemble neurons following defeat sessions 2, 5, and 8 in con (white, $n = 6–8$), res (blue, $n = 8–10$), and sus (red, $n = 6–8$) mice. *$p < .05$, **$p < .01$, effect test of group in 2-way analysis of variance followed by Tukey's multiple comparisons test. **(C)** Social ensemble size (con: $n = 6–8$, res: $n = 8–10$, sus: $n = 6–8$). *$p < .05$, effect test of group in 2-way analysis of variance followed by Tukey's multiple comparisons test. **(D)** Average percentage of reactivated dorsal CA1 neurons in defeat sessions 2, 5, and 8 (con: $n = 8$, res: $n = 10$, sus: $n = 7$). Histograms represent reactivations of (left) all recorded cells or (right) social ensemble neurons. All data are expressed as mean ± SEM. **(E)** Average percentage of reactivated dorsal CA1 neurons in the SIT (con: $n = 5–6$, res: $n = 10$, sus: $n = 5–6$). Histograms represent reactivations of (left) all recorded cells or (right) social ensemble neurons. All data are expressed as mean ± SEM. *$p < .05$, **$p < .01$, 1-way analysis of variance followed by Tukey's multiple comparisons test. con, control; CSDS, chronic social defeat stress; CSI, cosine similarity index; ns, not significant; res, resilient; SIT, social interaction test; sus, susceptible.

habituation to the revisited familiar CD1 mouse and lower preference toward the novel CD1 mouse than resilient mice. Therefore, CSDS impaired social memory for the aggressor strain, but the effect was greater in susceptible mice.

Lastly, a separate cohort of mice underwent a social novelty preference test prior to CSDS exposure and behavioral testing in the SIT (Figure 5C). It was found that stress-naïve mice with greater social novelty preference went on to show more interaction following CSDS with a CD1 mouse in the SIT (Figure 5D). Taken together, this finding suggests that stressed mice with lower interaction behavior in the SIT have preexisting impairments in social novelty memory.

DISCUSSION

Using a miniscope to longitudinally track hippocampal activity throughout CSDS, we identified differences in dCA1 representations of social interactions between susceptible and

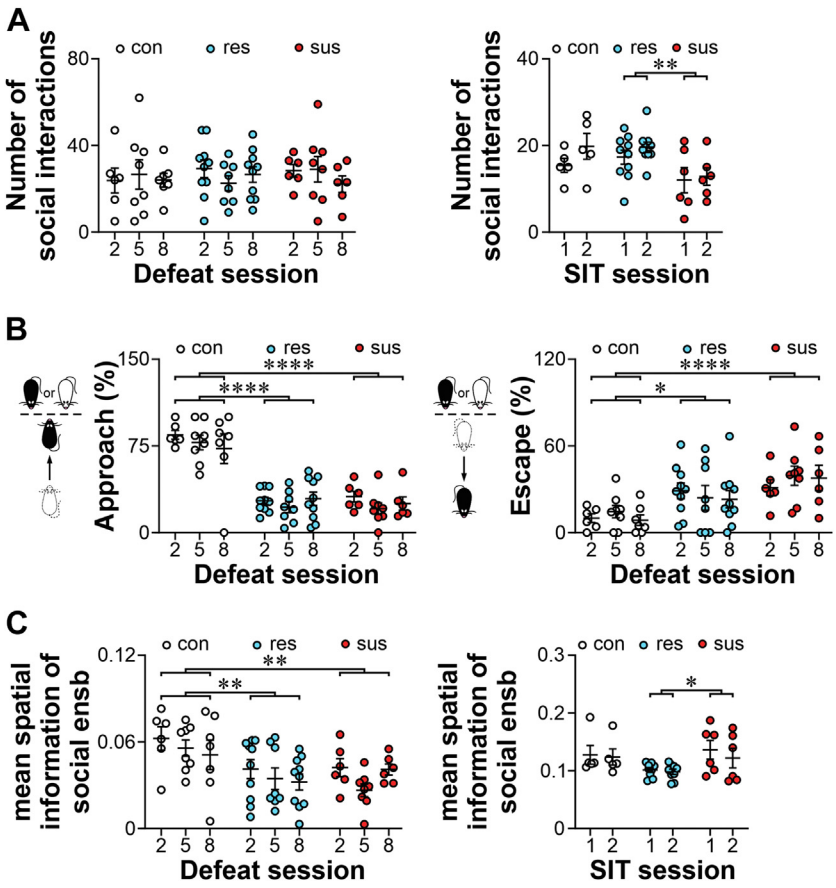

Figure 4. Social behavior and activity governed by spatial information do not account for decreased social ensemble fidelity in chronic social defeat stress susceptibility. **(A)** Number of social interactions (head distance < 10 cm and head angle ± 50°) with CD1 aggressors or same-strain control mice following defeat sessions 2, 5, and 8 in con (white) (n = 6–8), res (blue) (n = 8–10), and sus (red) (n = 6–8) mice. **(B)** Percentage of (left) approaches and (right) escapes initiated by C57BL/6 subject mice during chronic social defeat stress cohousing with CD1 aggressors or same-strain control mice (con: n = 6–8, res: n = 8–10, sus: n = 6–8). **(C)** Mean spatial information represented by dorsal CA1 neurons in the social ensemble (con: n = 6–8, res: n = 8–10, sus: n = 6–8). All data are expressed as mean ± SEM. *$p < .05$, **$p < .01$, ****$p < .0001$, effect test of group in 2-way analysis of variance followed by Tukey's multiple comparisons test. con, control; res, resilient; SIT, social interaction test; sus, susceptible.

resilient groups. When we examined population activity, we found that both the size and the information carried by social ensembles during CSDS cohousing were higher in resilient mice. Additionally, susceptible mice showed decreased social representation and memory for CD1 mice. Our findings suggest that differences in the processing of social information by the dCA1 may regulate stress susceptibility.

Prior reports from our group and others have examined hippocampal activity during the defeat period (6,8). Unlike previous studies, examining hippocampal activity during cohousing did not reveal greater reactivation in susceptible mice. This discrepancy may be largely due to differences in the stimuli inducing reactivation, which was physical attacks in the previous studies compared with social interactions in the current study. In addition, previous calcium imaging studies did not examine the effect of aggressor attacks on the activity of social ensembles (6). Future calcium imaging studies are needed to determine whether the reactivation of social ensembles during attacks are different in susceptible and resilient mice.

CSDS is a commonly used rodent model for the study of diverging responses to social stressors (7). Following identical stressors, the SIT can separate mice that are susceptible and express social avoidance from resilient mice that retain a greater level of social investigation (Figures S1 and S3). Susceptible and resilient mice shared behavioral similarities during CSDS cohousing (e.g., they appeared vigilant toward their neighboring aggressor). However, subtle differences were also found. Resilient mice maintained a shorter $Dist_{head}$ and $Angle_{head}$ to the CD1 aggressor than control mice during cohousing (Figure 1). When we compared the occupancy of A50, only susceptible mice showed a smaller $Angle_{head}$ to their cohoused neighbor than control mice, particularly following the last defeat episode (Figure 2). These findings support the importance of considering both head distance and heading direction toward social targets in the definition of social ensembles.

dCA1 spatial representations can be modulated by social processes and valenced experiences. dCA1 social place cells representing the location of social targets could support navigation processes through social environments (13,14). Recently, dCA1 activity in bats was shown to simultaneously represent spatial and social information (30). dCA1 neurons tuned to the relative distance between a subject and a conspecific were identified in instances where social presence was behaviorally important, such as the avoidance of collisions during bat flight (31). Spatial mapping is also influenced by valenced experiences, such that dCA1 place cells are biased to represent reward locations (32–34) and remap following an aversive experience (35). dCA1 neuron ensembles tuned to

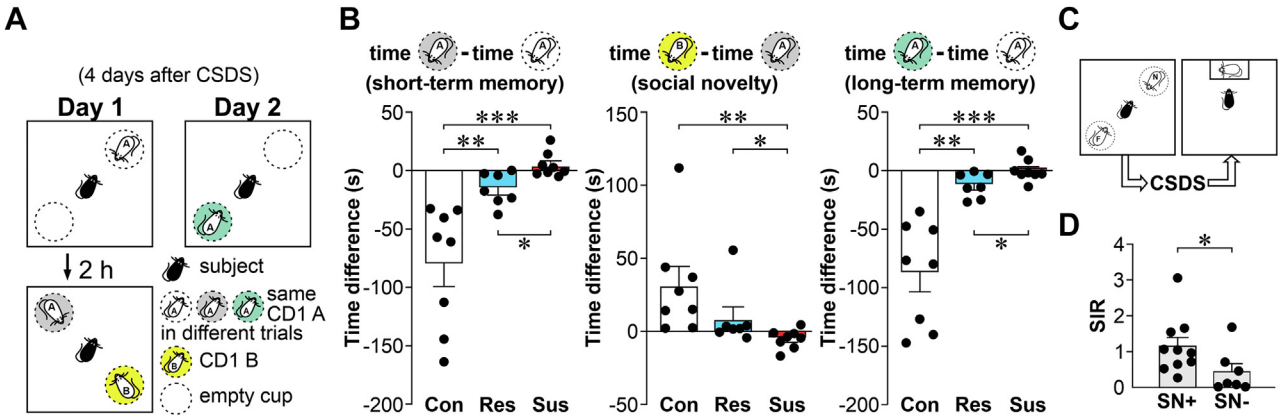

Figure 5. CSDS impairs social memory to a greater extent in susceptible mice. **(A)** Schematic of social memory tests. On day 1, subjects (defeated mice or nonstressed control mice) interacted with a novel CD1 A mouse (white) and an empty cup in an open field. Two hours later, subjects could investigate the now-familiar CD1 A mouse (light gray) or the novel CD1 B mouse (yellow). On day 2, subjects could investigate the familiar CD1 A mouse (green) or an empty cup. **(B)** Social memory performance in con (white) (n = 8), res (blue) (n = 7), and sus (red) (n = 8) mice. Left: short-term social memory measured as the time spent investigating the CD1 A mouse when it was familiar (2 hours) compared with novel. Middle: social novelty preference measured as the time spent investigating the novel CD1 B mouse compared with time spent investigating the familiar CD1 A mouse. Right: long-term social memory measured as the time spent investigating the CD1 A mouse when it was familiar (24 hours) compared with novel. All data are expressed as mean ± SEM. $^*p < .05$, $^{**}p < .01$, $^{***}p < .001$, Kruskal-Wallis test followed by Wilcoxon test. **(C)** Schematic of the experimental design: Subject mice underwent the social novelty test with the first session with 2 empty cups, the second session with one of these cups containing the familiar mouse, and the third session with the familiar and novel mice in different cups (only the third session is depicted). One day later, subject mice were stressed by CSDS for 8 days. One day later, stress susceptibility was determined by the social interaction test. Time subject mice spent in the second session (with a CD1 mouse)/time subject mice spent in the first session (empty cup) was used to calculate the SIR. **(D)** The SIR of subject mice that exhibited social novelty preference (i.e., showed a preference for the novel mouse in the social novelty test) (SN+) (n = 10) or no social novelty preference (i.e., showed a preference for the familiar mouse in the social novelty test) (SN−) (n = 7). All data are expressed as mean ± SEM. $^*p < .05$, Mann-Whitney test. con, control; CSDS, chronic social defeat stress; res, resilient; SIR, social interaction ratio; SN, social novelty; sus, susceptible.

aversive stimuli have also been identified (36). Finally, some studies have shown that dCA1 activity is required for identifying social targets that were associated with emotionally salient experiences (15,16). Here, we also uncovered differences in the dCA1 representation of social interactions in CSDS-susceptible and CSDS-resilient mice.

Compared with anatomical methods labeling active neurons (8,37), in vivo calcium imaging allows for increased temporal reliability, which enabled us to isolate neurons whose activity covaried with behavior. How these changes in dCA1 function contribute to CSDS susceptibility and resilience remains unclear. Following the second episode of CSDS, the activity of dCA1 social ensembles was reduced at a far distance from the social target in control and resilient mice only (Figure 3), supporting a reduction in social ensemble selectivity for close social interactions in susceptible mice. Social ensembles had increased CSI and greater size and reactivated more frequently in the SIT in resilient mice. Susceptible mice also exhibited lower reactivation of social ensembles in the SIT. These findings point to deficits in social information processing and memory in susceptible mice, which may be preexisting and indicate a vulnerability to social stress (Figure 5). In fact, impairments in spatial cognition have been reported following CSDS (38,39) and are accompanied by decreased hippocampal levels of proteins supporting memory functions (40).

The deficits in the dCA1 representation of social interaction may reduce social memory quality in susceptibility, thereby supporting memory generalization. CSDS has been shown to induce changes in dCA1 activity and contextual fear generalization (41). Despite both susceptible and resilient mice differentiating between CD1 and C57BL/6 mice in the SIT (Figure S4), susceptible mice showed greater difficulty recognizing novel versus familiar CD1 mice in the social memory test (Figure 5). Recent work has found that some susceptible mice show generalized fear toward CD1 mice and conspecifics (42), while sociability is preserved in CSDS-resilient mice interacting with novel strains, C57BL/6 adults, and juveniles, potentially attributable to the recognition of their nonthreatening nature (42–45). From literature on contextual fear conditioning, it has been suggested that poorer association between aversive stimuli and context could be a driving force for generalization. For example, context pre-exposure has been repeatedly shown to reduce context fear generalization (46,47). These findings led us to propose that diminished social representation and memory in susceptible mice may be a factor leading to higher and more generalized social fear.

We may draw parallels to hallmark memory deficits observed clinically in stress-related psychopathologies. Poor recollection of detailed autobiographical memory is a feature of depression and posttraumatic stress disorder (48). Similarly, fear generalization, or defensive responses triggered by incorrect assessments of imminent threat, is well described in posttraumatic stress disorder and anxiety (49). Together, these results suggest that it is possible that susceptible mice have increased memory for the negative CSDS event but that this memory is lacking specificity.

Importantly, investigations in female cohorts are warranted because stress-related psychopathology is more prevalent among women (50,51), presenting a limitation of the current study. CSDS models have typically been more challenging to implement in female cohorts due to a lack of consistent natural aggressive behavior among female mice. With the advent of

promising new defeat models in female mice, future studies related to social memory and information processing following social stress can be conducted with both sexes (52).

Conclusions

Our findings uncovered a role for hippocampal social cognitive processes in the individual variability of stress responses. CSDS resilience was characterized by greater social investigation of the aggressor strain and was accompanied by more reliable dCA1 correlates of social interaction and maintained social memory, while these changes were absent in susceptible mice, which instead showed diminished social memory for the aggressor strain. Therefore, susceptibility may manifest in mice through deficits in the processing and storage of social information.

ACKNOWLEDGMENTS AND DISCLOSURES

This work was supported by the Natural Sciences and Engineering Research Council of Canada (Grant No. RGPIN-2021-03739 [to TPW]) and the Canadian Institutes of Health Research (Grant No. PJ8 179866 [to TPW]).

AL and TPW were responsible for conceptualization. AL, TRZ, ASW, CYHF, XLYL, PS, BCMF, and TPW were responsible for methodology. AL, TRZ, ASW, XLYL, PS, and TPW were responsible for investigation. TPW was responsible for funding acquisition, project administration, and supervision. AL and TPW were responsible for writing the original draft of the article and reviewing and editing the article.

We thank the UCLA Miniscope team and Daniel Aharoni's laboratory for developing and sharing the miniscope technology. The current study used the services of the Molecular and Cellular Microscopy Platform at the Douglas Hospital Research Centre. Melina Jaramillo Garcia helped set up the imaging verification.

All data are available in the main text or the Supplement. Data are shared on Zenodo: https://zenodo.org/records/14647059. MATLAB codes are posted on GitHub: GitHub—tpwonglab/social-ensemble-analysis.

A previous version of this article was published as a preprint on bioRxiv: https://www.biorxiv.org/content/10.1101/2024.08.06.606823v1.

The authors report no biomedical financial interests or potential conflicts of interest.

ARTICLE INFORMATION

From the Integrated Program in Neuroscience, McGill University, Montreal, Quebec, Canada (AL, TRZ, PS); Neuroscience Division, Douglas Research Centre, Montreal, Quebec, Canada (AL, TRZ, ASW, CYHF, PS, TPW); School of Information Studies, McGill University, Montreal, Quebec, Canada (XLYL, BCMF); and Department of Psychiatry, McGill University, Montreal, Quebec, Canada (TPW).

Address correspondence to Tak Pan Wong, Ph.D., at takpan.wong@mcgill.ca.

Received Nov 19, 2024; revised Dec 27, 2024; accepted Jan 18, 2025.

Supplementary material cited in this article is available online at https://doi.org/10.1016/j.bpsgos.2025.100455.

REFERENCES

1. World Health Organization (2023): vol. 2024. Geneva: World Health Organization. Available at: https://www.who.int/news-room/fact-sheets/detail/depression. Accessed February 20, 2025.
2. Schmidt MV, Sterlemann V, Müller MB (2008): Chronic stress and individual vulnerability. Ann N Y Acad Sci 1148:174–183.
3. Larosa A, Wong TP (2022): The hippocampus in stress susceptibility and resilience: Reviewing molecular and functional markers. Prog Neuropsychopharmacol Biol Psychiatry 119:110601.
4. Fu CHY, Williams SCR, Cleare AJ, Brammer MJ, Walsh ND, Kim J, *et al.* (2004): Attenuation of the neural response to sad faces in major depression by antidepressant treatment: A prospective, event-related functional magnetic resonance imaging study. Arch Gen Psychiatry 61:877–889.
5. Hamilton JP, Gotlib IH (2008): Neural substrates of increased memory sensitivity for negative stimuli in major depression. Biol Psychiatry 63:1155–1162.
6. Anacker C, Luna VM, Stevens GS, Millette A, Shores R, Jimenez JC, *et al.* (2018): Hippocampal neurogenesis confers stress resilience by inhibiting the ventral dentate gyrus. Nature 559:98–102.
7. Krishnan V, Han MH, Graham DL, Berton O, Renthal W, Russo SJ, *et al.* (2007): Molecular adaptations underlying susceptibility and resistance to social defeat in brain reward regions. Cell 131:391–404.
8. Zhang TR, Larosa A, Di Raddo ME, Wong V, Wong AS, Wong TP (2019): Negative memory engrams in the hippocampus enhance the susceptibility to chronic social defeat stress. J Neurosci 39:7576–7590.
9. Trinkler I, King JA, Doeller CF, Rugg MD, Burgess N (2009): Neural bases of autobiographical support for episodic recollection of faces. Hippocampus 19:718–730.
10. Hitti FL, Siegelbaum SA (2014): The hippocampal CA2 region is essential for social memory. Nature 508:88–92.
11. Chiang MC, Huang AJY, Wintzer ME, Ohshima T, McHugh TJ (2018): A role for CA3 in social recognition memory. Behav Brain Res 354:22–30.
12. Okuyama T, Kitamura T, Roy DS, Itohara S, Tonegawa S (2016): Ventral CA1 neurons store social memory. Science 353:1536–1541.
13. Omer DB, Maimon SR, Las L, Ulanovsky N (2018): Social place-cells in the bat hippocampus. Science 359:218–224.
14. Danjo T, Toyoizumi T, Fujisawa S (2018): Spatial representations of self and other in the hippocampus. Science 359:213–218.
15. Lai WS, Ramiro LLR, Yu HA, Johnston RE (2005): Recognition of familiar individuals in golden hamsters: A new method and functional neuroanatomy. J Neurosci 25:11239–11247.
16. Kong E, Lee KH, Do J, Kim P, Lee D (2023): Dynamic and stable hippocampal representations of social identity and reward expectation support associative social memory in male mice. Nat Commun 14:2597.
17. Golden SA, Covington HE 3rd, Berton O, Russo SJ (2011): A standardized protocol for repeated social defeat stress in mice. Nat Protoc 6:1183–1191.
18. Pnevmatikakis EA, Giovannucci A (2017): NoRMCorre: An online algorithm for piecewise rigid motion correction of calcium imaging data. J Neurosci Methods 291:83–94.
19. Zhou P, Resendez SL, Rodriguez-Romaguera J, Jimenez JC, Neufeld SQ, Giovannucci A, *et al.* (2018): Efficient and accurate extraction of in vivo calcium signals from microendoscopic video data. eLife 7:e28728.
20. Mathis A, Mamidanna P, Cury KM, Abe T, Murthy VN, Mathis MW, Bethge M (2018): DeepLabCut: Markerless pose estimation of user-defined body parts with deep learning. Nat Neurosci 21:1281–1289.
21. Carrillo-Reid L, Lopez-Huerta VG, Garcia-Munoz M, Theiss S, Arbuthnott GW (2015): Cell assembly signatures defined by short-term synaptic plasticity in cortical networks. Int J Neural Syst 25:1550026.
22. Hamm JP, Peterka DS, Gogos JA, Yuste R (2017): Altered cortical ensembles in mouse models of schizophrenia. Neuron 94:153–167.e8.
23. Sheintuch L, Rubin A, Brande-Eilat N, Geva N, Sadeh N, Pinchasof O, Ziv Y (2017): Tracking the same neurons across multiple days in Ca^{2+} imaging data. Cell Rep 21:1102–1115.
24. Skaggs W, McNaughton B, Gothard K, Markus E (1997): An information-theoretic approach to deciphering the hippocampal code. Neural Inf Process Syst 5:1030–1037.
25. Wright EC, Hostinar CE, Trainor BC (2020): Anxious to see you: Neuroendocrine mechanisms of social vigilance and anxiety during adolescence. Eur J Neurosci 52:2516–2529.
26. Liang B, Zhang L, Barbera G, Fang W, Zhang J, Chen X, *et al.* (2018): Distinct and dynamic ON and OFF neural ensembles in the prefrontal cortex code social exploration. Neuron 100:700–714.e9.
27. Leake J, Zinn R, Corbit LH, Fanselow MS, Vissel B (2021): Engram size varies with learning and reflects memory content and precision. J Neurosci 41:4120–4130.
28. Tomar A, McHugh TJ (2022): The impact of stress on the hippocampal spatial code. Trends Neurosci 45:120–132.
29. Moy SS, Nadler JJ, Perez A, Barbaro RP, Johns JM, Magnuson TR, *et al.* (2004): Sociability and preference for social novelty in five inbred

strains: An approach to assess autistic-like behavior in mice. Genes Brain Behav 3:287–302.
30. Forli A, Yartsev MM (2023): Hippocampal representation during collective spatial behaviour in bats. Nature 621:796–803.
31. Sarel A, Palgi S, Blum D, Aljadeff J, Las L, Ulanovsky N (2022): Natural switches in behaviour rapidly modulate hippocampal coding. Nature 609:119–127.
32. Dupret D, O'Neill J, Pleydell-Bouverie B, Csicsvari J (2010): The reorganization and reactivation of hippocampal maps predict spatial memory performance. Nat Neurosci 13:995–1002.
33. Hollup SA, Molden S, Donnett JG, Moser MB, Moser EI (2001): Accumulation of hippocampal place fields at the goal location in an annular watermaze task. J Neurosci 21:1635–1644.
34. Sato M, Mizuta K, Islam T, Kawano M, Sekine Y, Takekawa T, *et al.* (2020): Distinct mechanisms of over-representation of landmarks and rewards in the hippocampus. Cell Rep 32:107864.
35. Blair GJ, Guo C, Wang S, Fanselow MS, Golshani P, Aharoni D, Blair HT (2023): Hippocampal place cell remapping occurs with memory storage of aversive experiences. eLife 12:e80661.
36. Barth AM, Jelitai M, Vasarhelyi-Nagy MF, Varga V (2023): Aversive stimulus-tuned responses in the CA1 of the dorsal hippocampus. Nat Commun 14:6841.
37. Okamura H, Yasugaki S, Suzuki-Abe H, Arai Y, Sakurai K, Yanagisawa M, *et al.* (2022): Long-term effects of repeated social defeat stress on brain activity during social interaction in BALB/c mice. eNeuro 9:ENEURO.0068-22.2022.
38. van der Kooij MA, Jene T, Treccani G, Miederer I, Hasch A, Voelxen N, *et al.* (2018): Chronic social stress-induced hyperglycemia in mice couples individual stress susceptibility to impaired spatial memory. Proc Natl Acad Sci U S A 115:E10187–E10196.
39. Wang H, Li F, Zheng X, Meng L, Chen M, Hui Y, *et al.* (2022): Social defeat drives hyperexcitation of the piriform cortex to induce learning and memory impairment but not mood-related disorders in mice. Transl Psychiatry 12:380.
40. Jianhua F, Wei W, Xiaomei L, Shao-Hui W (2017): Chronic social defeat stress leads to changes of behaviour and memory-associated proteins of young mice. Behav Brain Res 316:136–144.
41. Ren LY, Meyer MAA, Grayson VS, Gao P, Guedea AL, Radulovic J (2022): Stress-induced generalization of negative memories is mediated by an extended hippocampal circuit. Neuropsychopharmacology 47:516–523.
42. Ayash S, Schmitt U, Müller MB (2020): Chronic social defeat-induced social avoidance as a proxy of stress resilience in mice involves conditioned learning. J Psychiatr Res 120:64–71.
43. Li L, Durand-de Cuttoli R, Aubry AV, Burnett CJ, Cathomas F, Parise LF, *et al.* (2023): Social trauma engages lateral septum circuitry to occlude social reward. Nature 613:696–703.
44. Guo Q, Wang L, Yuan W, Li L, Zhang J, Hou W, *et al.* (2020): Different effects of chronic social defeat on social behavior and the brain CRF system in adult male C57 mice with different susceptibilities. Behav Brain Res 384:112553.
45. Cai DJ, Aharoni D, Shuman T, Shobe J, Biane J, Song W, *et al.* (2016): A shared neural ensemble links distinct contextual memories encoded close in time. Nature 534:115–118.
46. Keiser AA, Turnbull LM, Darian MA, Feldman DE, Song I, Tronson NC (2017): Sex differences in context fear generalization and recruitment of hippocampus and amygdala during retrieval. Neuropsychopharmacology 42:397–407.
47. Asok A, Hijazi J, Harvey LR, Kosmidis S, Kandel ER, Rayman JB (2019): Sex differences in remote contextual fear generalization in mice. Front Behav Neurosci 13:56.
48. Williams JMG, Barnhofer T, Crane C, Herman D, Raes F, Watkins E, Dalgleish T (2007): Autobiographical memory specificity and emotional disorder. Psychol Bull 133:122–148.
49. Dunsmoor JE, Paz R (2015): Fear generalization and anxiety: Behavioral and neural mechanisms. Biol Psychiatry 78:336–343.
50. Kessler RC, McGonagle KA, Swartz M, Blazer DG, Nelson CB (1993): Sex and depression in the National comorbidity Survey. I: Lifetime prevalence, chronicity and recurrence. J Affect Disord 29:85–96.
51. Tolin DF, Foa EB (2006): Sex differences in trauma and posttraumatic stress disorder: A quantitative review of 25 years of research. Psychol Bull 132:959–992.
52. Lopez J, Bagot RC (2021): Defining valid chronic stress models for depression with female rodents. Biol Psychiatry 90:226–235.